International Journal of Advances in Engineering and Management (IJAEM)
Volume 4, Issue 4 Apr 2022, pp: 257-264www.ijaem.net ISSN: 2395-5252

Radiation-Heterogeneous Processes inZrand Alloys Zr 1%Nb in Contact With Seawater

[1]Teymur Agayev, [*1]Gunel Imanova, [2]Imran Ali, [1]Salimkhan Aliyev, [1]Anar Aliyev,
[1]Ilaha Faradj-Zade, [3]Gunay Iskanderova, [4]Mail Tagiyev,
[4]Sevda Dzhafarova, [4]Arzu Ahmadova

[1]*Institute of Radiation Problems, Azerbaijan National Academy of Sciences, AZ 1143 - Baku, Azerbaijan*
[2]*Jamia Millia Islamia (Central University), New Delhi, 110025, India*
[3]*Institute of Physics, Azerbaijan National Academy of Sciences, AZ 1143 - Baku, Azerbaijan*
[4]*Azerbaijan State EconomicUniversity, Baku, AZ 1001 Azerbaijan*

Submitted: 01-04-2022 Revised: 06-04-2022 Accepted: 11-04-2022

ABSTRACT – The kinetics of accumulation of hydrogen during γ radiation on Zr and alloys Zr-1%Nbin contract with seawater at T = 300÷1273 K is investigated. The molecular hydrogen accumulation rates during radiation, thermal-radiation, and thermal processes in the Zr, Zr1%Nb alloys -SW system are determined. The contributions of thermal and radiation-heterogeneous processes during accumulation of molecular hydrogen and corrosion of Zr and alloys Zr1%Nbin contract with seawater is revealed.It has been established that under gamma irradiation of a system of zirconium and a Zr1% Nb alloy with seawater, with increasing temperature, the contribution of thermal processes of accumulation of molecular hydrogen also increases at T>1273 K, which prevail over radiation processes.

Key words:metallic zirconium, seawater, Zr, Zr1%Nb alloys, molecular hydrogen, γ- quanta.

I. INTRODUCTION

Atomic materials, radioactive isotopes, and different radiation-technology frameworks have as of late been broadly utilized in contact with seawater. Designing materials experience different sorts of radiation and contact with seawater. Inquire about into radiation-heterogeneous forms in building materials in contact with seawater permits one to uncover the impact of ionizing radiation on fabric erosion and amassing of atomic items of radiolysis of water within the encompassing environment[1-14].

Zirconium and zirconium combinations are broadly utilized as basic materials, center items of dynamic zone (AZ), water-cooled atomic control plants (NPP), which are worked beneath difficult conditions of radiation introduction, tall temperatures, warm and mechanical loads of the coolant and other unfavorable components. Resistance to these impacts generally decides the execution of the dynamic zone as a totally [1].

As can be seen from the writing information, radiation-heterogeneous forms in contact of to begin with radiation-oxidative treated zirconium and nano-zirconium oxide with water causes a alter within the sum of surface oxide film. The arrangement of an oxide film, in turn, changes the radiation-catalytic movement and physicochemical properties, which influence the dynamic parameters. One of them, the foremost delicate is the electro physical and optical properties of metal surfaces [18-26].

With this in intellect, we examined the radiation-heterogeneous of seawater decay and oxidation of fabric in contact with seawater at distinctive temperatures. Within the displayed work the comes about of considering the radiation-heterogeneous forms of decay of ocean water on the surface of metallic Zr and Zr1%Nb amalgam and the oxidation of these materials in contact with ocean water at distinctive temperatures beneath the activity of γ-quanta.

International Journal of Advances in Engineering and Management (IJAEM)
Volume 4, Issue 4 Apr 2022, pp: 257-264www.ijaem.net ISSN: 2395-5252

II. EXPERIMENTAL

Considers were carried out beneath inactive conditions in specialized quartz ampoules with V=1,0 $см^3$ [2,8,10]. Tests of reactor metallic zirconium and Zr1%Nb combinations within the shape of a lean lace were taken as the protest of ponder. The test weight of zirconium and Zr1%Nb combinations shifts within the run of 0.0798÷0.0825g. The contact surface of the tests was decided on the premise of geometric measurements and it is 8.47 sm^2/g and 9.05 sm^2/g for Zr, Zr1%Nb, individually.

In arrange to kill the commitment of outside natural matter on the stainless steel surface amid amassing of H_2, the tests were to begin with cleaned utilizing solvents (ethanol and acetone) and washed with refined water. This method was repasted three times; the tests were at that point dried at 300 – 320K in an dormant gas.Next, the samples were sealed in quartz ampoules and subjected to thermo vacuum treatment at 373 K and subsequently at 673 K, $P–10^{-2}$ Pa. the required amount at seawater was injected with a micro syringe. Seawater was collected from the Caspian Sea, 50m from the shore at a depth of 3m.

The composition of SW samples was studied by atomic-adsorption spectroscopy (ICP – MS Agilent 7700X),the results are listed in Table1. The weight of water injected into the ampoules was – 5.5×10^{-2} g. The accuracy of seawater injection into the ampoules was ± 2%. The ampoules containing the samples were demarcated until soluble oxygen and other gases (organic compounds) were removed from water by the freeze-pump-thaw cycle. Temperature during the experiments was maintained with an accuracy of$\pm1^0$C. The radiation and thermal-radiation processes were carried out using an isotopic source of ^{60}Co γ quanta. The intensity of the absorbed dose on the γ – radiation source was measured by chemical dosimeters (Ferro sulfate, cyclohexane and methane dosimeters) [13].

The analysis of hydrogen was performed on the US-made Agilent-7890A chromatograph in the following mode:column [2, 13].: C.-1010 P., 30mx0.53mm I.D. (25467), D. - TCD, C. Flow, F.-3 ml/min, 20Hz/.01 min, T(head)=500C, T(d.)=2300C, M. F.=0 ml/min, gas car. – Ar, oven: 500C(7.0 min), 200C/min to 2300C, i. temp..: 2300C.

III. RESULTS AND DISCISSION

Metal erosion was considered gravimetrically agreeing to the weight pick up of the tests some time recently and after the method. The reaching surface of the tests was decided agreeing to their geometric measure with at ± 10% precision. Radiolysis of seawater was carried out to uncover the impact of pollutions on radiolysis decay of seawater. Figure 1 appears the dynamic bend of amassing of atomic hydrogen upon radiolysis of unadulterated seawater.The rates and the radiation-chemical yield of molecular hydrogen upon radiolysis of seawater were determined based on the linear kinetic region; these values are $5{,}30\times10^{13}$molecules/gas and 0.81 molecules/100eV, respectively. The radiation-chemical yield upon radiolysis of pure water under identical conditions matches the published data and is 0,41÷0,45 molecules/100eV. The observed gain in the molecular hydrogen yield can be attributed to the contribution of dissolution of salts in water [12].

Organic impurities play no role, since neither carbohydrates, nor CO, nor CO_2 are observed among products. The contribution of inorganic salts Na^+, K^+, Mg^+ and Ca^+ captions in seawater can be explained by the effect of ion-dipole interactions between captions and water (Table 1) [16-17].

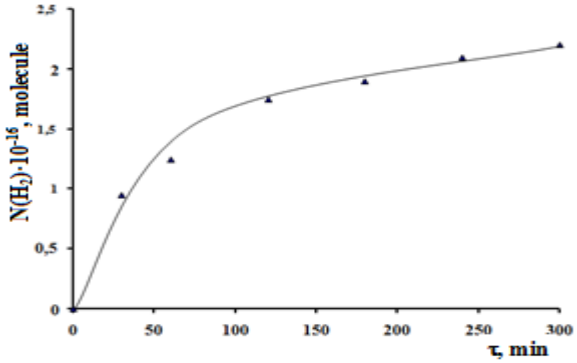

Fig.1. Kinetics of accumulation of molecular hydrogen during the radiolysis of sea water at T = 300K, D=1,05Gy/s

International Journal of Advances in Engineering and Management (IJAEM)
Volume 4, Issue 4 Apr 2022, pp: 257-264www.ijaem.net ISSN: 2395-5252

The interactions between captions and water dipoles shift the electron density from water molecules toward the acceptor levels of captions. The energy parameters of water, decomposition processes (ionization potential, bond energy) change due to this interaction [14,15].

Hence, the radiation-chemical yield of molecular hydrogen upon radiolysis of seawater is higher than that for radiolysis of our water.Radiolysis in the presence of Zr, Zr1%Nb was carried out elucidate the contribution of radiation-heterogeneous processes in radiolysis decomposition of seawater. The radiation-heterogeneous processes were conducted at a temperature range of 300 ÷1273K. The intensity of the absorbed radiation dose was calculated for the total Zr, Zr1%Nb alloys+SWsystem with allowance for the electron density of its components [16].

The number of hydrogen molecules supplied was calculated for the mass unit of the total system $Ni(H_2) = N_{H2}/m_{H2O} + m_{Zr}$ and the kinetic curves of accumulation $Ni(H_2) = f(t)$. Thermal decomposition of water was found to occur under the Zr, Zr1%Nb alloys + SW contact with increasing temperature of the process (above 473K).Hence, thermal and thermal radiation generation of hydrogen in the Zr, Zr1%Nb alloys + SW system was carried out under identical conditions at temperatures above 473K. the kinetic curves of accumulation of molecular hydrogen during radiation–heterogeneous (Fig.2a)and thermal (Fig.2b) decomposition of water in the Zr, Zr1%Nb alloys+ SW system are shown in Figs. 2a and 2b, respectively. The kinetic data were used to determine the rates and radiation chemical yields of hydrogen in these processes.

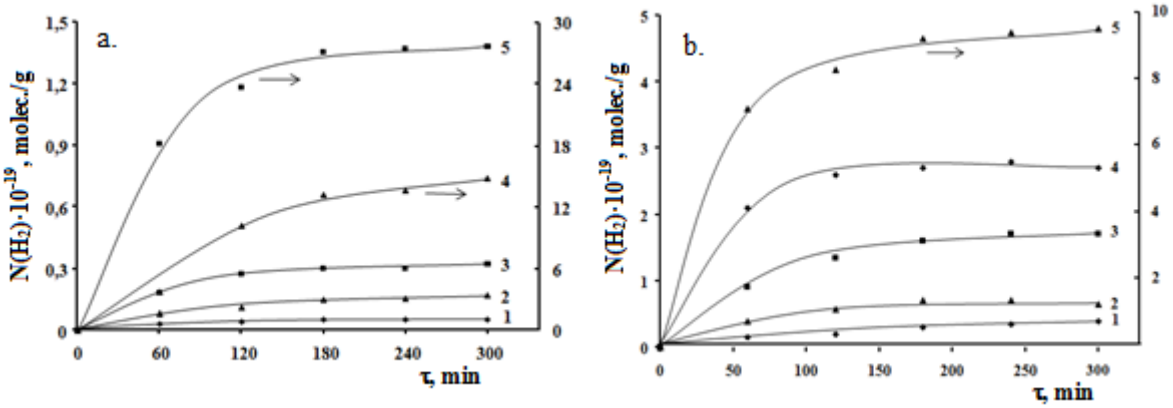

Fig.2. Kinetics of accumulation of molecular hydrogen during thermal (a) and radiation-thermal (b) decomposition of sea water on the surface of metallic zirconium at different temperatures: 1 – 473K; 2 – 573K; 3 – 673K; 4 – 773K; 5 – 1073K

The rates of radiation components during the thermal-radiation processes were calculated for the difference between the rates of thermal radiation and thermal processes of accumulation of molecular hydrogen:

$W_R(H_2) = W_{RT}(H_2) – W_T(H_2)$

Table 1.

Composition of seawater samples

Tested parameter	Unit	Results	Method applied
Temperatures	^{0}C	18,5	EPA170,0
Conductivity	ɲS/sm	192	EPA120,1
Salinity	%	11,58	SM2520B
Plant acids	%	98,3	ASTMD888B
Turbidity	NTU	7,93	EPA180,1
Aluminum	ɲg/L	112	EPA200,8
Antimony	ɲg/L	0,43	EPA200,8
Arsenic	ɲg/L	1,9	EPA200,8
Barium	ɲg/L	18,4	EPA200,8
Beryllium	ɲg/L	<0,03	EPA200,8
Boron	ɲg/L	2913	EPA200,8
Cadmium	ɲg/L	0,024	EPA7000B

International Journal of Advances in Engineering and Management (IJAEM)
Volume 4, Issue 4 Apr 2022, pp: 257-264www.ijaem.net ISSN: 2395-5252

Chromium	ng/L	351	EPA200,8
Cobalt	ng/L	0,335	EPA200,8
Copper	ng/L	0,159	EPA200,8
Iron	ng/L	1,6	EPA200,8
Lead	ng/L	161	EPA200,8
Magnesium	mg/L	0,953	EPA7000B
Manganese	ng/L	686	EPA200,8
Molybdenum	ng/L	7,73	EPA200,8
Nickel	ng/L	16,5	EPA200,8
Potassium	mg/L	0,18	ASTM D859-05
Selenium	ng/L	1,43	EPA200,8
Silver	ng/L	82,8	EPA200,8
Sodium	ng/L	<0,8	EPA200,8
Strontium	ng/L	<0,01	EPA200,8
Tellurium	ng/L	3116	EPA7000B
Tin	ng/L	9,92	EPA7000B
Uranium	ng/L	<0,3	EPA200,8
Zinc	ng/L	0,583	EPA200,8
Lithium	ng/L	6,43	EPA200,8
Vanadium	ng/L	4,09	EPA200,8
Gallium	ng/L	213	EPA200,8
Rubidium	ng/L	1,14	EPA200,8
Thallium	ng/L	5,14	EPA200,8
Ammonia	mg/L	9,24	EPA200,8
Bromide	mg/L	<0,01	EPA200,8
Chloride	mg/L	<0,02	SM4500-NOH3-Г
Fluoride	mg/L	3,9	ASTM D4327
Nitrate	mg/L	5393	ASTM D4327
Nitrite	mg/L	1,4	ASTM D4327
Phosphate	mg/L	0,021	SM4500-NO3-E
Quartz	mg/L	0,008	SM4500-NO2-B
Sulfate	mg/L	<0,02	EN1189-1996
Calcium	mg/L	3169	ASTMD4347

The kinetic parameters of thermal radiation, thermal and radiation processes are listed in Table 2.
The radiation-chemical yield and the hydrogen accumulation rate increase with temperature. The rates of thermal processes and water decomposition in contact with Zr, Zr1%Nb alloys increase as well.

Table 2.

Rates of radiation, radiation-thermal, thermal processes and radiation-chemical yields of molecular hydrogen during radiolysis decomposition of sea water in contact of Zr and Zr1%Nb alloys with sea water

№	T,K	$W_{RT}(H_2)$		$W_T(H_2)$		$W_R(H_2)$		$G(H_2)$, molec./100eV	
		molec./g·s							
		Zr	Zr1%Nb	Zr	Zr1%Nb	Zr	Zr1%Nb	Zr	Zr1%Nb
1.	300	-	-	-	-	$5,3\times10^{13}$	$6,1\times10^{13}$	0,81	0,93
2.	473	$9,44\times10^{14}$	$11,1\times10^{14}$	$4,25\times10^{14}$	$5,2\times10^{14}$	$5,19\times10^{14}$	$5,90\times10^{14}$	7,90	9,00

International Journal of Advances in Engineering and Management (IJAEM)
Volume 4, Issue 4 Apr 2022, pp: 257-264www.ijaem.net ISSN: 2395-5252

3.	**573**	$2{,}18 \times 10^{15}$	2.91×10^{15}	$1{,}1 \times 10^{15}$	$1{,}6 \times 10^{15}$	$1{,}08 \times 10^{15}$	$1{,}3 \times 10^{15}$	16,1	19,7
4.	**673**	$5{,}0 \times 10^{15}$	$6{,}1 \times 10^{15}$	$2{,}3 \times 10^{15}$	$2{,}8 \times 10^{15}$	$2{,}7 \times 10^{15}$	$3{,}3 \times 10^{15}$	39,5	48,1
5.	**773**	$1{,}02 \times 10^{17}$	$1{,}28 \times 10^{17}$	$5{,}8 \times 10^{16}$	$6{,}5 \times 10^{16}$	$4{,}2 \times 10^{16}$	$6{,}3 \times 10^{16}$	60,8	91,3
6.	**873**	$1{,}9 \times 10^{17}$	$2{,}6 \times 10^{17}$	$1{,}2 \times 10^{17}$	$1{,}35 \times 10^{17}$	$7{,}0 \times 10^{16}$	$1{,}25 \times 10^{17}$	101,4	181,1
7.	**1073**	$4{,}1 \times 10^{17}$	$6{,}5 \times 10^{17}$	$2{,}0 \times 10^{17}$	$3{,}5 \times 10^{17}$	$2{,}1 \times 10^{17}$	$3{,}0 \times 10^{17}$	304,3	434,7
8.	**1273**	$5{,}45 \times 10^{17}$	$6{,}9 \times 10^{17}$	$5{,}5 \times 10^{17}$	$6{,}83 \times 10^{17}$	-	-	-	-

Radiation-heterogeneous decomposition of water is the predominant process at temperatures T≤473K. The radiolysis processes of water decomposition in tis temperature range can be schematically presented as follows:

(1) Radiolysis of seawater under γ radiation:

$H_2O_s \rightarrow H_2 + \sum\Pi_i$, (1)

$W_R(H_2) = G(H_2)D \times 10^{-2}$

where H_2O_s is seawater, $\sum\Pi_i$ are other radiolysis products of seawater, $G(H_2)$ is the radiation-chemical yield of hydrogen and D is intensity of the absorbed dose of γ radiation.

(2) Formation of surface active states [10] and secondary electron emission [11] under γ radiation:

$HC \rightarrow S^* + e_{sec.}$ (2)

where S^* is the surface-active state and $e_{sec.}$are secondary electron emissions from the metal phase under irradiation.

(3) Decomposition of water molecules due to interaction with active states and $e_{sec.}$ generated due to:

$H_2O_s + S^* \rightarrow H_2 + \sum\Pi_i + S$ (3)

where S is the relaxed state of the surface active centers:

$H_2O_s + e_{sec} \rightarrow H_2 + \sum\Pi$ (4)

$W_3(H_2) = k_3[H_2O_s][S^*] + k_3[H_2O_s][e_{sec}]$

(4) Active sites are also accumulated on the surface of metal phases (Zr, Zr1%Nb) at T≥573K:

Zr, Zr1%Nb $\rightarrow S_T^*$(5)

$S_T^* + H_2O_s \rightarrow H_2 + \sum\Pi + S$ (6)

$W_T = k_T[S^*_T][H_2O_s]$

where S_T^* is the thermally activated state of the Zr, Zr1%Nb surface and S is the relaxed state of thermally activated states.

Thermal processes of generation of active site surface typically have an activation energy barrier and speed up with temperature. Taking into account the aforementioned stages of the radiation and thermal components of the processes, the equation for the molecular hydrogen accumulation rate can be written as follows:

$W(H_2) = G(H_2)D \times 10^{-2} + [H_2O](k_3[S^*_T] + k_4[e_{sec}])$

$W_T(H_2) = k_T[S_T^*[H_2O]]$

The relationship between the rates of the radiation and thermal components is:

$W_T(H_2)/W_{RT}(H_2) = G(H_2)D \times 10^{-2} / k_T[S_T^*[H_2O]] + k_3[S_T^*] + k_T[S_T^*] + k_4[e_{sec}]/k_T[S_T^*]$

Given that many parameters in these expressions are constant ($G(H_2)D \times 10^{-2}$ =5,30×10^{13}molecules/g.s.[H_2O]=const and the rate constant) the ratios between the rates of the radiation and thermal processes depend on surface concentration of active sites and the intensity of secondary electron emission from the metal. Increasing temperature stimulates the diffusion stages of radiation processes. The effect of temperature on radiation components of the processes are likely to occur in the temperature range where defect states migrate in the crystal lattice at T≥673K [11].

However, the rate of accumulation of thermally active sites increases with temperature and the results show that the thermal processes predominate over the radiation process $W_T \geq W_{RT}$, at T=1273K. Hence, neither the rates of the radiation components of the radiation–chemical yield of hydrogen can be determined at T≥1273K.

International Journal of Advances in Engineering and Management (IJAEM)
Volume 4, Issue 4 Apr 2022, pp: 257-264www.ijaem.net ISSN: 2395-5252

The rates of processes in the Arrhenius coordinates as a function of temperature were used to calculate the activation energies.

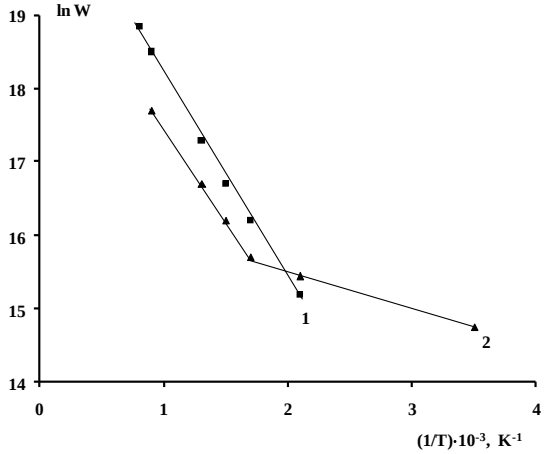

Fig.3. Temperature dependences of molecular hydrogen production during thermal (1) and radiation-thermal (2) processes in the system Zr + H_2O

Figure 3 shows the dependences of the rates of (2) thermal radiation, (3) thermal, (1) radiation processes of molecular hydrogen accumulation during radiation-heterogeneous decomposition of water in the presence of Zr, Zr1%Nb. The activation energies if thermal radiation and thermal processes of molecular hydrogen accumulation are 10,7and 38,5kJ/mol, respectively. The temperature curve for the rate of radiation processes contains two regions: the first one corresponds to T=300÷573K with E_a=10,7kJ/mol, while the second region corresponds to T=773÷1273K with E_g=38,5kJ/mol.It is clear that the activation energy of thermal decomposition of seawater in contact with Zr, Zr1%Nb is higher than that of thermal-radiation and radiation processes.

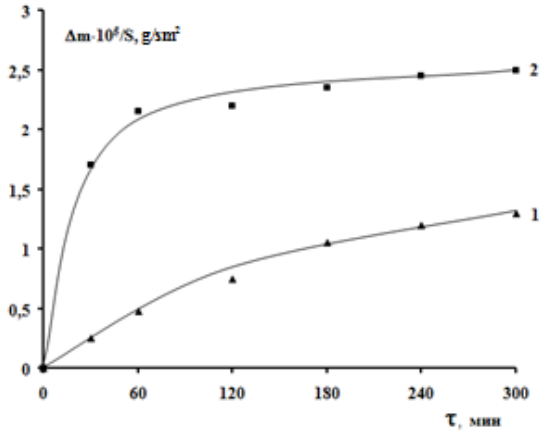

Fig.4. Kinetic curves of zirconium oxidation rates during (1) thermal and (2) radiation-thermal processes in contact with sea water

Radiation-generated active sites of the surface and secondary electron emissions, which have higher energy than thermally active sites, participate in radiation decomposition of seawater.In order to elucidate the regularities of surface processes, the kinetics of Zr, Zr1%Nb corrosion at T=673K was studied gravimetrically in the Zr, Zr1%Nb+SW system. Figure 4 shows the kinetic curves of stainless-steel corrosion during thermal and thermal-radiation processes. These curves were used to determine the rates of Zr, Zr1%Nb corrosion during thermal and thermal-radiation processes in contact with seawater (W_T=2,40·10^{-6} g/sm^2*s and W_{RT}=4,53·10^{-4} g/sm^2*s, respectively).

International Journal of Advances in Engineering and Management (IJAEM)
Volume 4, Issue 4 Apr 2022, pp: 257-264www.ijaem.net ISSN: 2395-5252

Zr, Zr1%Nb corrosion can be characterized both by the volume of molecular hydrogen and by the changesin sample weight after radiation, thermal-radiation and thermal processes in contact with SW. The kinetic curves showing changes in sample weight during the thermal-radiation processes are described by formula [2]:

$B(t) = B_{\infty}(1 - \exp(-k_c t))$,

where B_{∞} is concentration of products. In our experiments, which can be either oxide film or the amount of molecular hydrogen at $t \to \infty$, k_c – is the corrosion rate constant, $k_c = k_0 e^{-E_g/RT}$ [2], $k_0 = 10^{-2} s^{-1}$ and k_B is the Boltzmann constant.

The initial regions of the kinetic curves contain a linear dependence B(t) = f(t). In our experiments, the steady-state region in dependences $B_i = f(\tau)$ is observed at $\tau \geq 120$ min.

Thus, the following conclusions can be drawn:

- ✓ Soluble salts in seawater increase the radiation-chemical yield of molecular hydrogen as compared to pure water;
- ✓ Radiation heterogeneous processes in Zr, Zr1%Nb in contact with seawater increase the radiation-chemical yield of hydrogen and metal corrosion;
- ✓ When the temperature of radiation-heterogeneous processes is increased, thermal processes of generation of surface-active states (in addition to the radiation ones) occur at T ≥ 523.
- ✓ These processes contribute to water decomposition and metal oxidation;
- ✓ The contribution of radiation and thermal processes of water decomposition and Zr, Zr1%Nb corrosion in Zr, Zr1%Nb in contact with seawater has been determined.

The contribution of thermal processes increase under γ – radiation of the Zr, Zr1%Nb + SW systems with increasing temperature, at T≥1273 K, it predominates over the radiation contribution.

IV. CONCLUSIONS

The kinetics of accumulation of molecular hydrogen during γ radiolysis of sea and pure water has been studied. The radiation-chemical yield for seawater is higher ($G(H_2)$=0,81 molecules/100eV) than that during radiolysis of pure water ($G(H_2)$=0,45 molecules/100 eV). The kinetic of accumulation of molecular hydrogen and metal oxidation in radiation, thermal radiation and thermal processes in Zr, Zr1%Nb in contact with seawater (SW) have been studied. The generation of surface active sites and secondary electrons increases the rates of accumulation of molecular hydrogen and Zr, Zr1%Nb oxidation during the radiation and thermal radiation heterogeneous processes in the Zr, Zr1%Nb+SW system. Starting from T≥573K, thermal surface active sites of water decomposition and Zr, Zr1%Nb oxidation are accumulated in the metal phase during thermal radiation and thermal processes. The contribution of radiation and thermal processes during the radiation-heterogeneous processes in the Zr, Zr1%Nb+SW system has been determined. The contribution of thermal accumulation of molecular hydrogen increases during γ radiation of the Zr, Zr1%Nb+SW system with increasing temperature. It is dominant over the radiation processes at T≥1273K.

REFERENCES

[1]. Kobylyansky G.P. Dis. work.,Ulyanovsk, 2014, dis. for the degree of Doctor of Technical Sciences, 233 p.
[2]. Birks N., Mayer J. Introduction to high-temperature oxidation of metals. M.: Metallurgy, 1987. p.138.
[3]. Agaev T.N.,Garibov A.A., Kasumova U.M., Natural and technical sciences. 2012. No. 4. p.317.
[4]. Tomashov N.D., Chernova G.P. The theory of corrosion. M.: Metallurgy. 1993. p.57.
[5]. Kuznetsov A.M. Soros Educational Journal 2000. V.6.№5. p.45.
[6]. Grigoriev V.P. Soros educational journal 1999. No. 6. With. 62
[7]. Belousov V.V. Advances in Chemistry. 1998. V.7.p.631.
[8]. Nechaev A.F., PetrikN.G.,Sedov V.M., Sergeeva T.B., M.: 1988. p.54.
[9]. Agaev T.N., Ser. Physics of radiation damage and radiation materials science. 2009. No. 4. p. 202.
[10]. Gerasimov V.V., Corrosion of reactor materials. M.: Atomizdat, 1980. p.58.
[11]. Benard J. Oxidation of metals, M.: Metallurgy, 1968. p.320.
[12]. Ermolin V.I., Ivanova I.P., Knyazev D.I., et.al. Russ., J. Phys. Chem., A, 2012, vol. 86.3, p. 1029-1032
[13]. Agaev T.N., Metal science and heat treatment of metals. 2009. No. 1. p.49.
[14]. Pikaev A.K., Dosimetry in radiation chemistry. M.: Science. 1975. p.120.
[15]. NikulinaA.V.,Metal Science and heat treatment. Vol 45.p. 7-8. 2003.
[16]. ValovA.E.,VlasovM.G., GusachenkoE.I., StesikL.N., Physics of combustion and explosion, 1997, vol. 33, no. p.6.
[17]. AgayevT.N., Faradj–zade I. A., Aliyev A.G., Eyubov K.T., Aliyev S.M., Problems of atomic science and technology, 2017, №2 (108), p. 63-69.

[18]. Imanova G.T., Agayev T.N., Jabarov S.H., Investigation of structural and optical properties of zirconia dioxide nanoparticles by radiation and thermal methods, Modern Physics Letters B., 2021, 2150050-14.
[19]. Ali I., Imanova G.T., Garibov A.A., Agayev T.N., Jabarov S.H., Almalki A.SA., Alsubaie A., Gamma rays mediated water splitting on nano-ZrO_2 surface: Kinetics of molecular hydrogen formation, Radiation Physics and Chemistry, 2021, 109431.
[20]. T.N. Agayev, Sh.Z. Musayeva, G.T. Imanova, Studying the Kinetics of Formation of Molecular Hydrogen during the Radiolysis of Hexane and a Mixture of C_6H_{14}–H_2O on a Surface of n-ZrO_2, Russian Journal of Physical Chemistry A, 2021, 270–272.
[21]. Imran Ali, Gunel T. Imanova, X.Y. Mbianda, Omar M.L. Alharbid, Role of the radiations in water splitting for hydrogen generation, Sustainable Energy Technologies and Assessments, 51, 2022, 101926, 1-44.
[22]. Imanova G.T., Agaev T.N., Garibov A.A., Melikova S.Z., JabarovS.H..Akhundzada H.V., Radiation-thermocatalytic and thermocatalytic properties of n-ZrO_2-n-SiO_2 systems in the process of obtaining hydrogen from water at different temperatures, Journal of Molecular Structure, 2021, 130651.
[23]. G.T. Imanova, Kinetics Of Radiation-Heterogeneous And Catalytic Processes Of Water In The Presence Of Zirconia Nanoparticles, Advanced Physical Research, 2020, 94-101.
[24]. GunelTalatImanova and Mustafa Kaya, Importance of the Radiations in Radiolysis Processes for Hydrogen Generation, Book - Generis publishing, ISBN: 978-1-63902-693-7,2021, p. 50.
[25]. G.T. Imanova, Gamma Rays Mediated Hydrogen Generation By Water Decomposition On Nano-ZrO_2 Surface, Modern Approaches on Material Science, 2021, 508-514.
[26]. GunelImanova, Molecular hydrogen production by radiolysis of water on the surface of nano-ZrO_2 under the influence of gamma rays, Synthesis and Sintering, 2, 2022, 9–13.